Design of a Laboratory Borehole Storage model

Willem Mazzotti   **Yifeng Jiang**   **Patricia Monzó**   **Alberto Lazzarotto**
José Acuña   **Björn Palm**

ABSTRACT

This paper presents the design process of a 4x4 Laboratory Borehole Storage (LABS) model through analytical and numerical analyses. This LABS is intended to generate reference Thermal Response Functions (TRFs) as well as to be a validation tool for borehole heat transfer models. The objective of this design process is to determine suitable geometrical and physical parameters for the LABS. An analytical scaling analysis is first performed and important scaling constraints are derived. In particular, it is shown that the downscaling process leads to significantly higher values for Neumann and convective boundary conditions whereas the Fourier number is invariant. A numerical model is then used to verify the scaling laws, determine the size of the LABS, as well as to evaluate the influence of top surface convection and borehole radius on generated TRFs. An adequate shape for the LABS is found to be a quarter cylinder of radius and height 1.0 m, weighing around 1.2 tonnes. Natural convection on the top boundary proves to have a significant effect on the generated TRF with deviations of at least 15%. This convection effect is proposed as an explanation for the difference observed between experimental and analytical results in Cimmino and Bernier (2015). A numerical reproduction of their test leads to a relative difference of 1.1% at the last reported time. As small borehole radii are challenging to reproduce in a LABS, the effect of the borehole radius on TRFs is investigated. It is found that Eskilson's radius correction (1987) is not fully satisfactory and a new correction method must be undertaken.

INTRODUCTION AND LITERATURE REVIEW

Ground-source heat pump (GSHP) systems with vertical, closed-loop borehole heat exchangers (BHEs) are among the most energy-efficient systems for heating and cooling buildings, when properly designed. A key part in the design process of these systems is the borehole field sizing, performed in such a way that the secondary fluid circulating in the BHEs remains within pre-determined temperature limits over the lifetime of the installation. The long-term changes in secondary fluid temperature are predominantly influenced by heat transfer phenomena in the ground; accurately modelling these phenomena is thus important to reach a proper design. For a given borehole field geometry, a common method to calculate temperature changes over time is to use a Thermal Response Function (TRF) linking the increase in temperature at the borehole wall to a given, constant heat rate and given ground properties.

TRFs and ground heat transfer modelling. Broadly-cited TRFs are Eskilson's g-functions (1987) which are dependent on similarity parameters of the borehole field, namely, $r_b^* = r_b/H$, $B^* = B/H$, and $t^* = t/t_s = 9Fo$. Eskilson's g-functions may be defined by $T_b - T_0 = \frac{\bar{q}}{2\pi\lambda} g(r_b^*, B^*, t^*)$ which relates the temperature increase at the borehole wall, $T_b - T_0$, to the specific heat injection rate, $\bar{q}$, and the thermal conductivity, λ. Eskilson generated g-functions numerically, assuming that all borehole walls in the field have the same temperature, which is additionally uniform with depth.

Claesson and Eskilson (1987) furthermore introduced an analytical solution based on uniform heat injection along a Finite-Line-Source (FLS) in a semi-infinite medium, which was later discussed and developed by other authors (Cui et al., 2006; Javed & Claesson, 2011; Lamarche, 2011; Lamarche & Beauchamp, 2007; 2002). Although convenient for fast computation, the different FLS methods failed to reproduce Eskilson's g-functions for large borehole fields because of the difference in boundary conditions (BCs) applied along the borehole wall between the two models. Although none of these BCs duly represent a real case, g-functions will better represent temperature changes in the borehole field when

all boreholes are fed in parallel, as highlighted by Cimmino et al. (2013). This FLS vs. g-function issue was tackled by several authors who proposed modelling straight (Cimmino & Bernier, 2014) and inclined (Lazzarotto, 2016; Lazzarotto & Björk, 2016) boreholes as stacks of FLS while imposing a uniform temperature BC. Cimmino (2015) coupled such as stack-FLS mode to a quasi-steady-state borehole heat transfer model, thereby moving the BC outside of the boreholes, allowing to impose the same inlet temperature for all boreholes in the field.

Besides Eskilson (1987), other authors have numerically generated TRFs. A novel approach to numerically model borehole fields using a highly conductive material (HCM) was presented by Monzó et al. (2015) and later improved (Monzó, 2018). Other numerical models have been developed but are not discussed here.

Experimental and monitoring work. As highlighted in the previous section, many authors have focused on developing analytical and numerical models or methods to predict temperature changes in borehole fields, with the aim to improve the accuracy of GSHP design. However, due to the slow transitory nature of heat transfer phenomena in long boreholes, long-term experimental and monitoring studies have been scarce. This has been emphasized in the literature (Cimmino & Bernier, 2015; Cullin et al., 2015; Montagud et al., 2011; Spitler & Bernier, 2011, 2016). Spitler & Bernier (2016) identified the relevance and usefulness of long-term monitoring of thermally unbalanced borehole fields.

Some installations have been monitored over longer periods of 1 to 5 years (Cullin et al., 2015; Montagud, Corberán, Montero, & Urchueguía, 2011; Yavuzturk & Spitler, 2001) although none of the studies has been used to validate ground heat transfer models. In fact, validation of ground heat transfer models in real systems is harden by the long time scale involved. Moreover, uncontrolled or unknown parameters such as groundwater flow, thermal properties or geological conditions may complicate the validation process in real installations. Practical difficulties such as data gaps, unknown control strategies or lack of documentation may also arise. Additionally, uncertainties are hard to assess in operating systems and rarely reported.

An alternative is to perform lab experiments in small-scale physical models. Such laboratory apparatuses are attractive because the time scale is reduced and the tests can be performed in a controlled environment. A lab-scale apparatus was successfully built by Cimmino and Bernier (2015) based on a previous work (Salim Shirazi & Bernier, 2014). The authors obtained an experimental TRF that could be compared to a semi-analytical method. In the reviewed literature, this is the only attempt to validate ground heat transfer models on the long-term. A discrepancy between the experimental TRF and the analytical one was observed, although the difference is comprised within the measurement uncertainty at a 95% confidence level (Cimmino & Bernier, 2015). The authors proposed an explanation for this observed difference based on the air temperature variation above the tank, though the proposed correction did not fully succeed in reproducing the observations. The present article proposes another explanation for the difference based on scaling laws and natural convection. Other lab-scale models were constructed although their use was limited to analysis of short-term models or other purposes (Beier et al., 2011; Eslami-nejad & Bernier, 2012; Hellström & Kjellsson, 2000; Kramer et al., 2015).

This article presents the design process and sizing of a LABS simulating multiple vertical BHEs. The design process is based on an analytical scaling analysis as well as a numerical model which is a modified version of the model presented by Monzó et al. (2015). Additionally, some technical, practical and uncertainty limitations are used as constraints to determine the different design parameters.

METHODOLOGY

The main goal of this work is to determine adequate dimensions, materials and conditions for the LABS, which was preliminary thought as a vertical cylindrical container filled with a material simulating the ground and in which boreholes are placed at the center as shown in Figure 1. This figure also includes important parameters to be determined under the design process. The first step in this scaling process is to ensure that the solutions obtained with the LABS will be the same as for the real-scale model. A general analytical analysis of the effect of downscaling on the heat transfer phenomena is thus performed at first. Then, the borehole field to model is chosen, as well as the LABS size and related time scale. A preliminary selection of materials must also be performed before numerical simulations can be performed. Although seemingly sequential, the design procedure has consisted of many iterations and cross-investigations.

Scaling analysis

Some scaling requirements may be obtained analytically by stating the governing equations for the real and lab-scale cases. Assuming constant and uniform thermal properties, the two heat equations may be written, respectively, as

$$\frac{1}{\alpha}\frac{\partial T}{\partial t} = \frac{1}{r}\frac{\partial}{\partial r}\left(r\frac{\partial T}{\partial r}\right) + \frac{1}{r^2}\frac{\partial^2 T}{\partial \varphi^2} + \frac{\partial^2 T}{\partial z^2} \text{ and } \frac{1}{\alpha'}\frac{\partial T'}{\partial t'} = \frac{1}{r'}\frac{\partial}{\partial r'}\left(r'\frac{\partial T'}{\partial r'}\right) + \frac{1}{r'^2}\frac{\partial^2 T'}{\partial \varphi'^2} + \frac{\partial^2 T'}{\partial z'^2} \quad (1)$$

Note that the apostrophe symbol is be used to refer to the lab-scale parameters and variables. For similar Initial Condition (IC) and Boundary Conditions (BCs), the behavior of the real and lab-scale cases will be the same if the governing equations are the same. By introducing a proportional and isotropous geometrical scaling factor, β, a thermal diffusivity scaling factor, γ, as well as a time scaling factor, τ, such that

$$\beta = \frac{r}{r'} = \frac{z}{z'} = \frac{H}{H'} \quad ; \quad \tau = \frac{t}{t'} \quad ; \quad \gamma = \frac{\alpha}{\alpha'} \quad (2)$$

and applying the corresponding change of variables to the first eq. in 1, the latter may be rewritten as

$$\frac{\beta^2}{\alpha\tau}\frac{\partial T}{\partial t'} = \frac{1}{r'}\frac{\partial}{\partial r'}\left(r'\frac{\partial T}{\partial r'}\right) + \frac{1}{r'^2}\frac{\partial^2 T}{\partial \varphi'^2} + \frac{\partial^2 T}{\partial z'^2} \quad (3)$$

Note that $\varphi = \varphi'$ and that an anisotropic scaling would set requirement for an anisotropic material in the LABS, which is difficult to achieve. For similar IC and a set of BCs, the 2nd eq. in 1 and eq.3 have the same solution if $\frac{\beta^2}{\alpha\tau} = \frac{1}{\alpha'}$ which is equivalent to the invariance of the Fourier number: $Fo_r = \frac{\alpha t}{r^2} = \frac{\alpha' t'}{r'^2} = Fo_{r'}$ or $Fo_H = Fo_{H'}$. Therefore, as expected, the Fourier number must be conserved, constituting a first scaling requirement. One of the advantages of downscaling becomes clear from the previous eq., as τ is proportional to β, which takes large values ($\beta \gg 1$).

As previously mentioned, the IC and BCs must also be analogous in order to obtain the same solution in the real and LABS cases. Dirichlet BCs will not be affected by the downscaling as opposed to Neumann and convective BCs. Such BCs may arise at the borehole wall, as well as the bottom and top boundaries. At the borehole wall, a Neumann BC is expressed as $-\lambda\frac{\partial T}{\partial r}(r_b, z, t) = \frac{q}{2\pi r_b}$, $\forall(z,t) \in \left([D;H] \times \mathbb{R}^{+*}\right)$, where D is the buried depth. Applying the same change of variable as for the heat equation, one obtains $q' = q \cdot \frac{\lambda'}{\lambda}$, constituting a second requirement. Hence, the linear heat flux is slightly modified when downscaling.
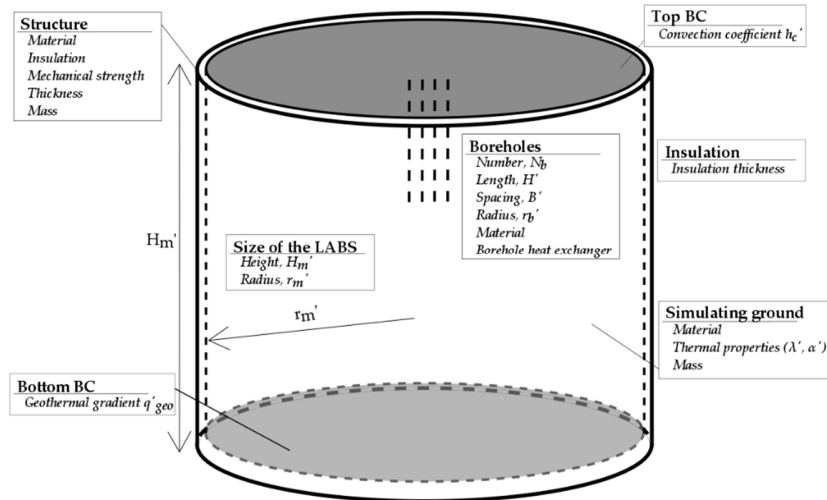

Figure 1. Preliminary outline of the lab-scale model (LABS) including important design parameters to be determined

Similarly, relations may be obtained for the geothermal heat flux BC and the top convective BC

$$\frac{\lambda'}{\lambda}\beta q_{geo} = q'_{geo} \quad \text{and} \quad \frac{\lambda'}{\lambda}\beta h_c = h'_c \tag{4}$$

Eq.4 also become requirements if the BC applied at the top and bottom of the model are a convective and a Neumann BC, respectively. The β appearing in eq.4 implies large increases in the equivalent geothermal heat flux and convection coefficient when downscaling the model ($\beta \gg 1$). For instance, a 300 m deep borehole field modelled by a 0.5 m LABS will lead to $\beta = 600$. Assuming a natural convection coefficient of 10 W·m⁻²·K⁻¹ on top of a real-scale system, the required convection on top of LABS would be of 6000 W·m⁻²·K⁻¹ for equal thermal conductivities. Thus, forced convection will likely be required at the top of the LABS to reproduce the behavior of real-scale installations having natural convection as top BC. Note that radiation is considered to be accounted for in the convection coefficient.

It is later shown that a Neumann BC with a typical natural convection coefficient of 10 W·m⁻²·K⁻¹ leads to similar results than a Dirichlet BC in the real-size case but not in the LABS case.

Choice of the borehole field to be modelled and sizing criteria for the LABS

Borehole field to be modelled. In order to perform a downscaling, the geometry of the real-scale borehole field must be set. A 4x4 borehole field has been arbitrarily chosen with the intention to observe thermal interactions between boreholes. Since TRFs only depend on non-dimensional geometrical parameters (r_b^*, B^* and $D^* = D/H$) for a given configuration, only those values need to be chosen in theory. However, for the purpose of the design, a borehole field with the following fixed geometrical parameters is chosen as a starting point for the downscaling process: $H = 300$ m, $r_b = 5.75$ cm and $D = B = 5$ m corresponding to $r_b^* = 1.92 \cdot 10^{-4}$, $B^* = D^* = 1.67 \cdot 10^{-2}$.

Sizing criteria for the LABS. The sizing of the LABS consists of two parts. The 1st one is the determination of β or, in other words, H' while the 2nd part is the determination of the dimensions of the LABS, H'_m and r'_m. H' is set as 50 cm, corresponding to $\beta = 600$, because this leads to a test duration of about a few days, which is what is wanted. The test duration is determined as the time at which the solution approach asymptotic condition (eq.6). A H' value of 50 cm is also considered a reasonable size for laboratory facilities although it implies reaching a challenging 0.11 mm for r'_b, given the parameters chosen in the previous paragraph. This radius issue is discussed later in the paper.

The dimensions of the LABS must be designed so that it fits in laboratory facilities; the maximum allowable size is thus arbitrarily set as 1.8 m in height and width. The size also affects the LABS mass that may be significant. To exactly determine the required dimensions of the LABS for $\beta = 600$, sizing criteria must be defined. The LABS boundaries should influence as least as possible conduction in the simulating ground over the test duration. Since the main goal of the LABS is to generate and validate TRFs, the sizing criteria may arbitrarily be defined as

$$\left|\overline{\Delta T}(r_b, t_{ss}) - \overline{\Delta T_{ref}}(r_b, t_{ss})\right| < 0.5 \cdot U(T, 95\%) \tag{5}$$

where $\overline{\Delta T_{ref}}(r_b, t_{ss})$ is the depth-integral mean of the temperature increase at the borehole wall at the end of the test, t_{ss}, emanating from a reference model with a large domain; thus one in which the boundaries negligibly influence the TRF. $U(T, 95\%)$ is the expanded uncertainty of temperature measurement at the borehole wall at a 95% confidence level. The targeted value for $U(T, 95\%)$ is 0.5 K. The criterion expressed in eq.5 is arbitrary but the aim is to limit the uncertainty in the determination of the TRF. Note that the test duration is chosen for the evaluation of criterion 5 because this is when the boundary effects will be the largest. The following criterion is thus used to determine t_{ss}

$$\forall t > t_{ss}, \frac{\left|\overline{\Delta T_{ref}}(r_b, t) - \overline{\Delta T_{ref}}(r_b, t_{ss})\right|}{\overline{\Delta T_{ref}}(r_b, t)} < 0.5\% \tag{6}$$

Lab-Scale Numerical Model (LSNM) and choice of materials

LSNM. To find the LABS dimensions that suit criterion 5, a Lab-Scale Numerical Model (LSNM) is used. A

real-scale numerical model is also built to verify the scaling laws found in previous sections. Both numerical models are an adaptation of Monzó et al. (2015). It is chosen to use a numerical tool instead of an analytical one for flexibility reasons, for instance in the type of BCs applied. Notably, the top and bottom BCs can be shifted between Dirichlet or convective BC, and geothermal heat flux or adiabatic condition, respectively. All vertical boundaries are adiabatic. The LSNM simulates the 4x4 borehole field presented earlier but symmetry is used to reduce the model to a 1/8 of the original domain. Analytical analyses were also undertaken but are not presented here.

Simulating ground. The simulating ground refers to the material in the LABS, as opposed to the simulated ground that refers to the real-scale material. The thermal properties of the simulating ground are of primary importance since they directly influence the heat diffusion process in the LABS. Indeed, a larger thermal diffusivity in the model will lead to shorter test durations but the heat plume will reach further away from the boreholes, thereby increasing the required LABS size. A lower thermal conductivity will on the other hand lead to a larger temperature increase that may create some practical problems. Another important feature of the simulating ground is its interchangeability, which is why saturated sand is chosen as simulating ground. The thermal properties assumed for the simulated and simulating ground are as follow: $\lambda = 3.5$ W·m^{-1}·K^{-1}, $\alpha = 1.58 \cdot 10^{-6}$ m^2·s^{-1} and $\lambda' = 3.0$ W·m^{-1}·K^{-1}, $\alpha' = 7.00 \cdot 10^{-7}$ m^2·s^{-1}, respectively (Arkhangelskaya & Lukyashchenko, 2017; Sundberg, 1991; Tarnawski et al., 2011). The thermal properties of the simulating ground should be well characterized before experiments are to be performed.

Structure and insulation. For practical reasons, steel was chosen as a structural material. Since steel has a relatively high thermal conductivity, the container should be thermally isolated from the ground to avoid thermal disturbances. An insulation layer is thus needed between the steel and the simulating ground. This insulation layer moreover reduces the potential thermal influence from the environing air as well as heat losses. Although not presented here, a 2D steady-state numerical model is used to assess the impact of the insulation thickness on the heat losses. The used thermal conductivity and heat transfer coefficient are of 0.035 W·m^{-1}·K^{-1} and 10 W·m^{-2}·K^{-1}, respectively.

Establishment of initial temperature gradient

The establishment of the initial temperature gradient in the LABS from a uniform ambient temperature may be significantly long as compared to the actual test duration. A LSNM is used to assess the establishment time. The time needed for the establishment of the initial gradient may also be estimated analytically by superposing the solutions for 1D conduction in two semi-infinite solids which intersection corresponds to any vertical cross-section of the LABS. Each semi-infinite solid is applied a constant heat flux on the boundary surface, the heat fluxes being equal in magnitude but of opposite sign for each solid. Taking a reference depth at the mid-depth of the LABS and defining $z^+ = H'_m/2 + z$ and $z^- = H'_m/2 - z$, the temperature increase may be expressed as such, for $Fo < 0.2$

$$\Delta T = q_{geo} \cdot \frac{H'_m}{\lambda} \left(\frac{2}{\sqrt{\pi}} \sqrt{Fo} \left(e^{-\frac{z^{+2}}{4\alpha t}} - e^{-\frac{z^{-2}}{4\alpha t}} \right) + z^- \cdot erfc\left(\frac{z^-}{2\sqrt{\alpha t}}\right) - z^+ \cdot erfc\left(\frac{z^+}{2\sqrt{\alpha t}}\right) \right) \tag{7}$$

RESULTS AND DISCUSSIONS

Verifications on the real-scale numerical model

The real-scale numerical model is not validated per say but several verifications have been performed in order to ensure the reliability of the results. In this part, the model has Dirichlet and adiabatic BCs at the top and bottom boundaries, respectively. The first verification regards the steady-state distribution of heat flow between boreholes which is in accordance with that of Cimmino (2015). The second verification performed is a comparison between the LSNM, the Infinite Line Source (ILS) and Lazzarotto and Björk (2016). Results from the LSNM are in accordance with those two analytical models (only at early times for the ILS). The largest relative difference between Lazzarotto and Björk and the numerical g-function is of 4.0% at $ln(t/t_s) = -5.5$. This difference tends to be reduced when a finer discretization is used for the stacked-FLS model of Lazzarotto and Björk (40 elements are used).

Real-scale numerical model vs LSNM

In order to verify the scaling relations expressed previously, the real-scale numerical model presented in the previous section is compared to a LSNM, with similar geometry but different thermal properties. Note that thermal properties do not affect TRFs but are important in downscaling the BC. $\beta = 600$ is used leading to $r'_m = H'_m = 1.4$ m and $H' = 50$ cm. Geothermal heat flux is applied to both the real-scale numerical model and the LSNM. Geothermal heat flux means an initial vertical temperature gradient making the determination of the g-function not formally possible. However, a TRF may be defined in a similar way as $T_b - \overline{T_0} = \frac{\overline{q}}{2\pi\lambda} TRF(r_b^*, B^*, D^*, t^*)$. The TRFs obtained for each model are presented in Figure 2. The maximum absolute relative difference between the TRF obtained with the real-scale model and with the LSNM is of 15% at early times. The difference is lower than 2.6% after $ln(t/t_s) = -12$, corresponding to 16 hours in the real-scale application. This relative difference shows a decreasing trend as time increases, reaching values as low as 0.05 % towards the simulation end. The LSNM thus give very similar result to the real-scale numerical model on the long-term.

Ground dimension of the LABS

The ground dimension of the LABS is determined according to the criteria given in eq.5-6. A LSNM with the same scaling factor as previously used ($\beta = 600$) but of radius and height 5 m is used to generate the reference solution mentioned in eq.5-6. This reference solution is then utilized to determine t_{ss}. It is found that t_{ss} is about 131.8 hours (5.5 days). This corresponds to a non-dimensional logarithmic time, $ln(t_{ss}/t_s)$, of 2.48. LSNMs of different dimensions are then run to find a size matching the criterion expressed in eq.5.

Each model has equal radius and height. The resulting differences in borehole average temperature between the reference solution and the solutions for the different LSNM sizes are shown in Figure 3. These differences are shown for two different dimensionless times corresponding to the two different colored sets of points in the figure. The limit in criterion 5 is also represented by the black dashed line. The smallest model that satisfies eq.5 has a height and radius of 1 m. This model has an average borehole temperature 0.19 K higher than the reference model at $ln(t_{ss}/t_s) = 2.48$. The difference increases to 0.72 K at $ln(t_{ss}/t_s) = 4$. The sand mass for such a model would be around 4.9 tons. Nevertheless, in the same way as the LSNM domain can be reduced to a 1/8 cylinder by applying symmetry, the LABS size may be reduced as to limit its weight. It is chosen to reduce the LABS to a 1/4 cylinder in order to avoid the physical modelling of half boreholes. The sand mass is then reduced to 1.2 tons.

Challenges with the borehole radius

A problem arising from the chosen scale factor ($\beta = 600$) is that the borehole radius becomes very small in the LABS: r'_b indeed turns out as 0.2 mm, which is challenging to reproduce in a physical model.
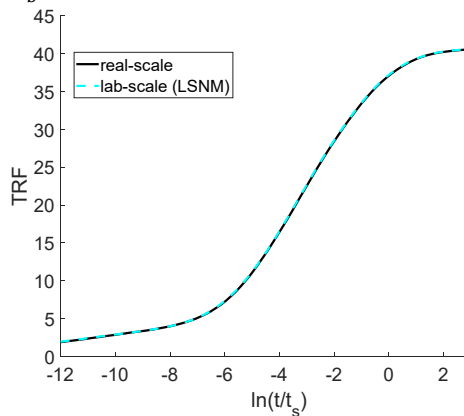

Figure 2. TRFs for real-scale and LSNM for a 4x4 borehole field with $r_b^* = 1.92 \cdot 10^{-4}$ and $B^* = D^* = 0.0167$
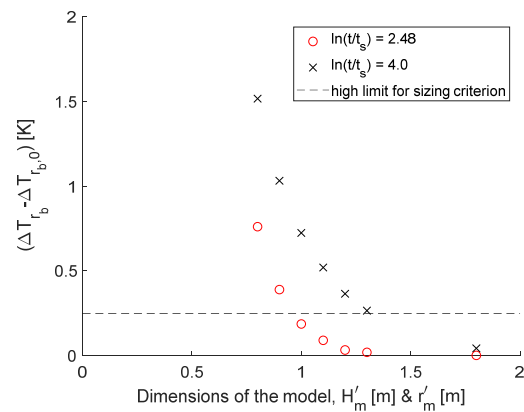
Figure 3. Difference in borehole average temperature between the reference solution and the solutions for different model sizes. The height, H'_m, and radius, r'_m, are equal.

As the results are scale-independent, one could decrease β in order to increase the borehole radius. This would however lead to unrealistic dimensions for the LABS: a borehole radius of 2 mm would for instance mean a LABS of 10 m in radius and height. This issue could be bypassed by considering that the LABS simulates shorter boreholes, thereby reducing β. The limits of this method may, however, be noted as the increase in borehole radius is directly proportional to the reduction in borehole depth; a 2 mm borehole radius in the LABS would then limit the simulated real-scale borehole depth to about 30 m. Another method is to use a correction factor such as the one suggested by Eskilson (1987),

$$g(r_1^*, B^*, t^*) = g(r_2^*, B^*, t^*) + \ln(r_2^*/r_1^*) \tag{8}$$

which is derived by assuming steady-state radial conduction between the two radii. This approximation may be valid for small differences in radius but axial effects may become important for larger ones, leading to underestimated values of the TRF for large times. On the contrary, the correction will lead to overestimated values of the TRF for short times, when the quasi-steady-state regime has not yet been established between the two considered radii. These two features can be observed in Figure 4 that shows the numerically-generated TRF for three different r_b^* in graph (a), while graph (b) shows the same TRF corrected with eq.8. Note that a more accurate correction factor could be derived from analytical or numerical analysis but this is left to a later stage of the project. Anyhow, experimentally-obtained TRF for a given r_b^* would allow the determination of other TRF corresponding to different r_b^* values.

Influence of the top convective BC

As noted in previous sections, the convection heat transfer coefficient, h_c, at the top boundary layer must be scaled up when downscaling the borehole field. Values of h_c around 10 W·m^{-2}·K^{-1} can be expected at the top of real size borehole fields, corresponding to a h_c' of 5142 W·m^{-2}·K^{-1} given the chosen scale factor and thermal conductivities. The latter value is challenging to achieve; hence, the influence of h_c' and, thus, h_c, is evaluated using the LSNM in order to assess the possible deviations in TRF for lower h_c', namely 514.2, 51.42 and 5.142 W·m^{-2}·K^{-1} corresponding to h_c of 1, 0.1 and 0.01 W·m^{-2}·K^{-1}. Note that the ambient temperature is set as 0°C.

The resulting TRFs are shown in Figure 5 together with the TRF obtained for constant temperature BC at the top. As could be expected, decreasing h_c' leads to increasing TRF values. At $\ln(t/t_s) = 4$, relative differences with the TRF generated with constant temperature BC are of 0.4%, 3.1%, 15.4% and 54.2% for h_c' of 5142, 514.2, 51.42 and 5.142 W·m^{-2}·K^{-1}, respectively. It may be observed that a h_c of 10 W·m^{-2}·K^{-1} in a real size borehole field ($h_c' = 5142$ W·m^{-2}·K^{-1} in the LABS) leads to an almost identical TRF than with the constant temperature BC.
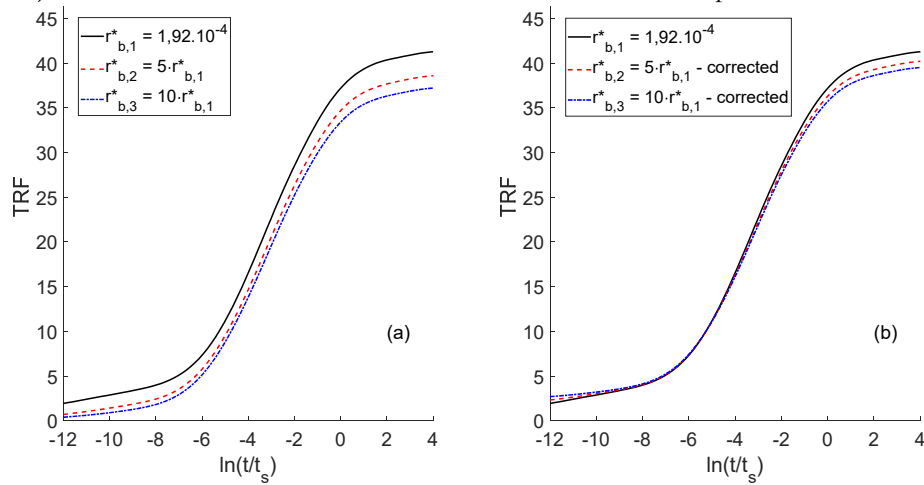

Figure 4. Influence of the borehole radius-to-depth aspect ratio on the numerically generated TRF for a 4x4 borehole field: (a) without correction, (b) with Eskilson's correction

A h'_c, of 514.2 W·m⁻²·K⁻¹ leads to a reasonable error while being easier to achieve than 5142 W·m⁻²·K⁻¹. A value of 514.2 W·m⁻²·K⁻¹, or higher, can be reached by circulating constant temperature water in micro-channels or by using a phase-change material (Kim et al., 2017). Note that the diverging TRF for h_c = 5.142 W·m⁻²·K⁻¹ is due to the finite size of the LSNM, the adiabatic BC on the sides and the close-to-adiabatic BC at the top.

As previously noted, the top BC appears to have been left uncontrolled in Cimmino and Bernier (2015), entailing natural convection on the surface. In those conditions, one may expect h'_c values between 1 to 6 W·m⁻²·K⁻¹. Considering radiation, heat transfer coefficients could go up to 15 W·m⁻²·K⁻¹ (Bergman et al., 2011). A LSNM reproducing as faithfully as possible the conditions reported by Cimmino and Bernier (2015) is made using values of h'_c of 1 and 10 W·m⁻²·K⁻¹, as well as a Dirichlet BC on top. The results are shown in Figure 6 which also displays results for h'_c = 10 W·m⁻²·K⁻¹ and borehole radii changing by ± 0.5 mm due to the uncertainty on the actual borehole radius used during the tests. A convection coefficient of 10 W·m⁻²·K⁻¹ seems to reproduce fairly well the behavior observed during their test with differences of 3.5% and 1.1% at the first and last reported time points, respectively. This could thus be one of the reasons for the observed discrepancy between the experimental and analytical results in Cimmino and Bernier (2015).

Heat losses and establishment of initial temperature gradient

Heat losses through vertical plates. Heat losses through the side of the LABS have so far been disregarded but it is important to limit those losses as much as possible to improve accuracy. A 2D steady-state model of the LABS corner is used with the radial temperature from the LSNM at 0.5 m depth and $ln(t/t_s)$ = 4.4 as the inner BC and a heat transfer coefficient of 10 W.m⁻².K⁻¹ as outer BC. The maximum relative heat loss is found to be 8.2% and 3.8% for 5 cm and 10 cm insulation thickness, respectively, as compared to the heat injected in the LABS. Although this calculation represents a worst-case scenario, the losses are relatively high. This could be improved by adding insulation on the outer part of the metallic structure as well as reducing the radiation losses using a low-emissivity layer. The corner of the LABS should be particularly well-insulated as the temperature there will be higher and the heat losses will moreover directly affect the thermal response because of the direct proximity with the boreholes.

Establishment of initial temperature gradient. Using the analytical model described previously, it is found that the steady-state condition is reached after about 70 hours. This, however, corresponds to an ideal situation in which an extraction heat flux of same magnitude as the geothermal heat flux can be maintained at the surface. A numerical simulation shows that the time for establishment of the initial temperature gradient keeping a constant temperature at the top BC could be as long as 30 days. Hence, the establishment of the initial temperature gradient may be a time-consuming process that ought to be optimized to reduce test duration. Similarly, the recovery period – not studied here – could be optimized to avoid long waiting time between tests.
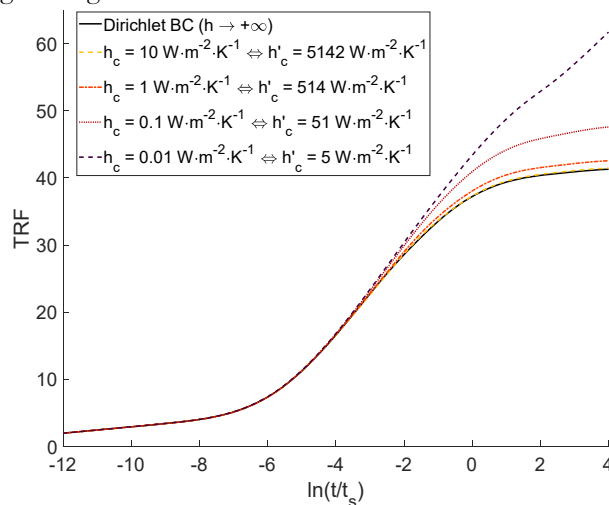

Figure 5. Influence of the top BC convection heat transfer coefficient on the TRF for 4x4 borehole field

CONCLUSION

The dimensioning of LAboratory-scale Borehole Storage (LABS)with 4x4 boreholes was investigated in this study; first by deriving scaling laws from an analytical analysis and then through the use of a numerical model. The analytical analysis shows that the invariance of the Fourier number is a requirement and that Neumann or convective boundary conditions (BC) are scaled up proportionally to the geometrical scaling factor, when downscaling. This BC scale-up is notably proposed as a possible explanation for the observed discrepancy between experimental and analytical results in Cimmino and Bernier (2015). A numerical reproduction of their experiment indeed shows a good agreement with their test results when natural convection is accounted for: the relative difference in Thermal Response Functions (TRFs) is of 1.1% at the last reported time.

It is found that, for the considered LABS, natural convection as top BC leads to TRF values at least 15% higher than those obtained with a Dirichlet BC. Therefore, forced convection or PCM must be used on the top BC to accurately reproduce real-scale TRFs.

The geometrical downscaling factor is fixed as 600, leading to scaled borehole depth of 50 cm and a test duration of about 5.5 days. For this configuration, a radius and height of both 1.0 m are found to be appropriate dimensions for the LABS, which is assumed of cylindrical shape. For these dimensions, the borehole temperature increase induced by boundary effects is indeed less than 0.25 K, which is half the expected uncertainty of temperature measurements. Symmetry is used to reduce the LABS to a ¼ cylinder, thereby reducing its weight to 1.2 instead of 4.9 tonnes.

The scaling laws found through the analytical analysis are confirmed through numerically modelling real-scale and laboratory scale borehole fields. The relative differences in TRFs between the two models is lower than 2.6%.

As small borehole aspect ratios are challenging to reproduce in a LABS, the effect of the borehole radius on TRFs is numerically investigated and it is found that Eskilson's radius correction (1987) is not fully satisfactory. A new correction method based on analytical or numerical analysis must be undertaken.

Heat losses as high as 8.2% of the total injected power are found to possibly occur towards the end of the tests, even with 5 cm insulation. This stresses the need for a larger insulation layer and/or the use of a low-emissivity layer on the outer shell of the LABS. The time needed for the establishment of the temperature gradient in the LABS is found to be at least 70 hours and may be as long as a month. The LABS should be optimized so that this duration and the time needed for recovery are as short as possible.

Future work includes the prediction and minimization of uncertainties, design of the measurement system and the system to implement on top of the LABS, testing of the simulating sand, as well as the construction of the LABS.
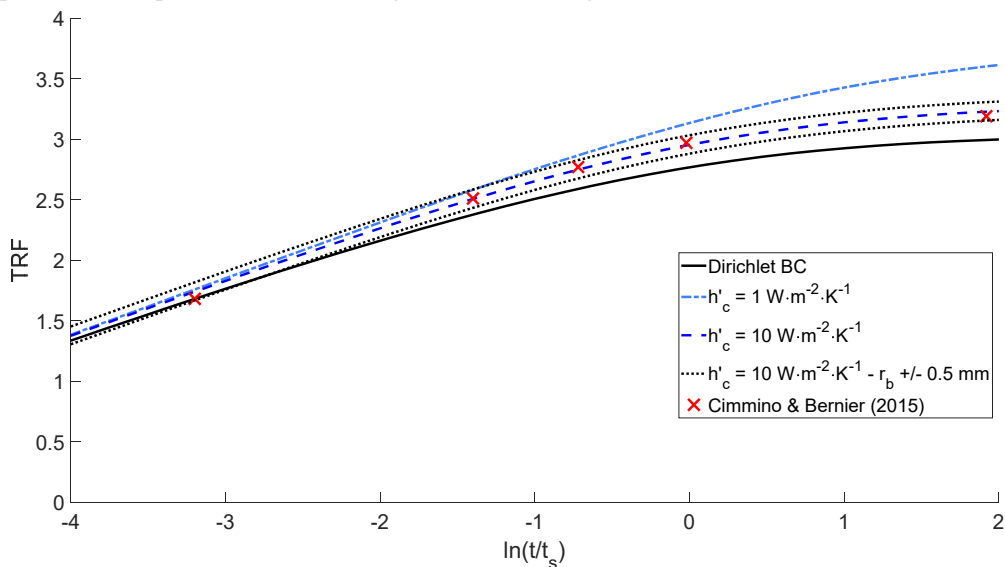

Figure 6. Numerical reproduction of the test performed by Cimmino and Bernier (2015)

ACKNOWLEDGMENTS

NOMENCLATURE

B = Borehole spacing (m)
D = Buried depth (m)
Fo = Fourier number (-)
g = G-function (-)
H = Active borehole depth (m)
h = Convection / global heat transfer coefficient ($W \cdot m^{-2} \cdot K^{-1}$)
q = Specific heat rate ($W \cdot m^{-1}$) or heat flux ($W.m^{-2}$)
r = Radius (m)
T = Temperature (°C or K)
t = Time (s)
z = Depth (m)
α = Thermal diffusivity ($m^2 \cdot s^{-1}$)
β = Spatial scale factor (-)
γ = Thermal diffusivity scale factor (-)
λ = Thermal conductivity ($W \cdot m^{-1} \cdot K^{-1}$)
φ = Azimuth angle (°)

Subscripts

b = borehole
c = convection
m = model or LABS
geo = geothermal
s = characteristic time
ss = test duration (asymptotic time)
0 = initial

Superscripts

$'$ = relative to the LABS
$*$ = dimensionless parameter
$\bar{x}$ = integral mean of x

REFERENCES

Arkhangelskaya, T., & Lukyashchenko, K. (2017). Estimating soil thermal diffusivity at different water contents from easily available data on soil texture, bulk density, and organic carbon content. Biosystems Engineering. https://doi.org/10.1016/j.biosystemseng.2017.06.011

Beier, R. A., Smith, M. D., & Spitler, J. D. (2011). Reference data sets for vertical borehole ground heat exchanger models and thermal response test analysis. Geothermics, 40(1), 79–85. https://doi.org/10.1016/j.geothermics.2010.12.007

Bergman, T. L., Lavine, A. S., Incropera, F. P., & Dewitt, D. P. (2011). Fundamentals of heat and mass transfer (7th ed). Hoboken, NJ: Wiley.

Cimmino, M. (2015). The effects of borehole thermal resistances and fluid flow rate on the g-functions of geothermal bore fields. International Journal of Heat and Mass Transfer, 91, 1119–1127. https://doi.org/10.1016/j.ijheatmasstransfer.2015.08.041

Cimmino, M., & Bernier, M. (2014). A semi-analytical method to generate g-functions for geothermal bore fields. International Journal of Heat and Mass Transfer, 70, 641–650. https://doi.org/10.1016/j.ijheatmasstransfer.2013.11.037

Cimmino, M., & Bernier, M. (2015). Experimental determination of the g-functions of a small-scale geothermal borehole. Geothermics, 56, 60–71. https://doi.org/10.1016/j.geothermics.2015.03.006

Cimmino, M., Bernier, M., & Adams, F. (2013). A contribution towards the determination of g-functions using the finite line source. Applied Thermal Engineering, 51(1–2), 401–412. https://doi.org/10.1016/j.applthermaleng.2012.07.044

Claesson, J., & Eskilson, P. (1987). Conductive Heat Extraction by a Deep Borehole. Analytical Studies. (Technical Report). Lund: University of Lund.

Cui, P., Yang, H., & Fang, Z. (2006). Heat transfer analysis of ground heat exchangers with inclined boreholes. Applied Thermal Engineering, 26(11), 1169–1175. https://doi.org/10.1016/j.applthermaleng.2005.10.034

Cullin, J. R., Spitler, J. D., Montagud, C., Ruiz-Calvo, F., Rees, S. J., Naicker, S. S., … Southard, L. E. (2015). Validation of vertical ground heat exchanger design methodologies. Science and Technology for the Built Environment, 21(2), 137–149. https://doi.org/10.1080/10789669.2014.974478

Eskilson, P. (1987, June). Thermal analysis of heat extraction boreholes. Lund University, Sweden.

Eslami-nejad, P., & Bernier, M. (2012). Freezing of geothermal borehole surroundings: A numerical and experimental assessment with applications. Applied Energy, 98, 333–345. https://doi.org/10.1016/j.apenergy.2012.03.047

Hellström, G., & Kjellsson, E. (2000). Laboratory Measurements of Heat Transfer Properties for Different Types of Borehole Heat Exchangers. In Proc. of Terrastock. Stuttgart, Germany.

Javed, S., & Claesson, J. (2011). New analytical and numerical solutions for the short-term analysis of vertical ground heat exchangers. ASHRAE Transactions, 117(1), 3.

Kim, Y., Kim, M., Ahn, C., Kim, H. U., Kang, S.-W., & Kim, T. (2017). Numerical study on heat transfer and pressure drop in laminar-flow multistage mini-channel heat sink. International Journal of Heat and Mass Transfer, 108, 1197–1206. https://doi.org/10.1016/j.ijheatmasstransfer.2016.12.025

Kramer, C. A., Ghasemi-Fare, O., & Basu, P. (2015). Laboratory Thermal Performance Tests on a Model Heat Exchanger Pile in Sand. Geotechnical and Geological Engineering, 33(2), 253–271. https://doi.org/10.1007/s10706-014-9786-z

Lamarche, L. (2011). Analytical g-function for inclined boreholes in ground-source heat pump systems. Geothermics, 40(4), 241–249. https://doi.org/10.1016/j.geothermics.2011.07.006

Lamarche, L., & Beauchamp, B. (2007). A new contribution to the finite line-source model for geothermal boreholes. Energy and Buildings, 39(2), 188–198. https://doi.org/10.1016/j.enbuild.2006.06.003

Lazzarotto, A. (2016). A methodology for the calculation of response functions for geothermal fields with arbitrarily oriented boreholes – Part 1. Renewable Energy, 86, 1380–1393. https://doi.org/10.1016/j.renene.2015.09.056

Lazzarotto, A., & Björk, F. (2016). A methodology for the calculation of response functions for geothermal fields with arbitrarily oriented boreholes – Part 2. Renewable Energy, 86, 1353–1361. https://doi.org/10.1016/j.renene.2015.09.057

Montagud, C., Corberán, J. M., Montero, Á., & Urchueguía, J. F. (2011). Analysis of the energy performance of a ground source heat pump system after five years of operation. Energy and Buildings, 43(12), 3618–3626. https://doi.org/10.1016/j.enbuild.2011.09.036

Monzó, P. (2018). Modelling and monitoring thermal response of the ground in borehole fields (PhD Thesis). KTH Royal Institute of Technology, Stockholm, Sweden. Retrieved from http://urn.kb.se/resolve?urn=urn:nbn:se:kth:diva-222007

Monzó, P., Mogensen, P., Acuña, J., Ruiz-Calvo, F., & Montagud, C. (2015). A novel numerical approach for imposing a temperature boundary condition at the borehole wall in borehole fields. Geothermics, 56, 35–44. https://doi.org/10.1016/j.geothermics.2015.03.003

Salim Shirazi, A., & Bernier, M. (2014). A small-scale experimental apparatus to study heat transfer in the vicinity of geothermal boreholes. HVAC&R Research, 20(7), 819–827. https://doi.org/10.1080/10789669.2014.939553

Spitler, J., & Bernier, M. (2011). Ground-source heat pump systems: The first century and beyond. HVAC&R Research, 17(6), 891–894. https://doi.org/10.1080/10789669.2011.628221

Spitler, J., & Bernier, M. (2016). 2 - Vertical borehole ground heat exchanger design methods. In S. J. Rees (Ed.), Advances in Ground-Source Heat Pump Systems (pp. 29–61). Woodhead Publishing. https://doi.org/10.1016/B978-0-08-100311-4.00002-9

Sundberg, J. (1991). Termiska egenskaper i jord och berg (No. 12). Swedish Geotechnical Institute.

Tarnawski, V. R., Momose, T., & Leong, W. H. (2011). Thermal Conductivity of Standard Sands II. Saturated Conditions. International Journal of Thermophysics, 32(5), 984–1005. https://doi.org/10.1007/s10765-011-0975-1

Yavuzturk, C., & Spitler, J. D. (2001). Field validation of a short time step model for vertical ground-loop heat exchangers / Discussion. ASHRAE Transactions; Atlanta, 107, 617.

Zeng, H. Y., Diao, N. R., & Fang, Z. H. (2002). A finite line-source model for boreholes in geothermal heat exchangers. Heat Transfer?Asian Research, 31(7), 558–567. https://doi.org/10.1002/htj.10057